Determination of temperature dependency of material parameters for lead-free alkali niobate piezoceramics by the inverse method

K. Ogo, K. Kakimoto, M. Weiß, S. J. Rupitsch, and R. Lerch

Citation: AIP Advances **6**, 065101 (2016); doi: 10.1063/1.4953327
View online: http://dx.doi.org/10.1063/1.4953327
View Table of Contents: http://scitation.aip.org/content/aip/journal/adva/6/6?ver=pdfcov
Published by the AIP Publishing

Determination of temperature dependency of material parameters for lead-free alkali niobate piezoceramics by the inverse method

K. Ogo,[1] K. Kakimoto,[2,a] M. Weiß,[3] S. J. Rupitsch,[3] and R. Lerch[3]
[1]*Department of Materials Science and Engineering, Nagoya Institute of Technology, Gokiso-cho, Showa-ku, Nagoya 466-8555, Japan*
[2]*Frontier Research Institute for Materials Science, Nagoya Institute of Technology, Gokiso-cho, Showa-ku, Nagoya 466-8555, Japan*
[3]*Chair of Sensor Technology, Friedrich-Alexander-Universität of Erlangen-Nürnberg, Paul-Gordan-Str. 3/5, 91052 Erlangen, Germany*

(Received 10 April 2016; accepted 22 May 2016; published online 3 June 2016)

Sodium potassium niobate (NKN) piezoceramics have been paid much attention as lead-free piezoelectric materials in high temperature devices because of their high Curie temperature. The temperature dependency of their material parameters, however, has not been determined in detail up to now. For this purpose, we exploit the so-called Inverse Method denoting a simulation-based characterization approach. Compared with other characterization methods, the Inverse Method requires only one sample shape of the piezoceramic material and has further decisive advantages. The identification of material parameters showed that NKN is mechanically softer in shear direction compared with lead zirconate titanate (PZT) at room temperature. The temperature dependency of the material parameters of NKN was evaluated in the temperature range from 30 °C to 150 °C. As a result, we figured out that dielectric constants and piezoelectric constants show a monotonous and isotropic increment with increasing temperature. On the other hand, elastic stiffness constant c_{44}^E of NKN significantly decreased in contrast to other elastic stiffness constants. It could be revealed that the decrement of c_{44}^E is associated with an orthorhombic-tetragonal phase transition. Furthermore, ratio of elastic compliance constants s_{44}^E/s_{33}^E exhibited similar temperature dependent behavior to the ratio of piezoelectric constants d_{15}/d_{33}. It is suspected that mechanical softness in shear direction is one origin of the large piezoelectric shear mode of NKN. Our results show that NKN are suitable for high temperature devices, and that the Inverse Method should be a helpful approach to characterize material parameters under their practical operating conditions for NKN. [http://dx.doi.org/10.1063/1.4953327]

I. INTRODUCTION

Piezoelectric materials are used in many electric devices, especially sensors and actuators.[1,2] Currently, the most popular piezoelectric materials are lead-based piezoceramics, for example lead zirconate titanate $Pb(Zr,Ti)O_3$ (PZT) piezoceramics because of their excellent piezoelectric properties. However, lead has been concerned as a harmful element for environment as well as humans. Therefore, lead-free piezoelectric materials have been paid a lot of attention.[3–9] Sodium potassium niobate $(Na,K)NbO_3$ (NKN) piezoceramics are a highly-promising candidate for lead-free piezoelectric materials in high temperature devices because of their high Curie temperature (T_C~>400 °C),[3–6,10–13] which is higher than that of PZT piezoceramics (T_C~350 °C).

[a]Electronic mail: kakimoto.kenichi@nitech.ac.jp

For practical applications of piezoelectric materials, numerical simulations are commonly used to predict mechanical and electrical behavior of sensors and actuators under operating conditions. As a matter of principle, precise numerical simulation results demand reliable material parameters. In general, material parameters are provided by resonance-antiresonance method.[14] In this method, several kinds of sample shapes are needed to determine material parameters. In addition, resonance ultrasound spectroscopy was used as an approach for material parameters. In these method, only one sample shape is sufficient for determination materials parameters.[15] In this study, we identify material parameters of NKN by means of the Inverse Method. The Inverse Method is a simulation-based approach and provides material constants by minimizing deviations between frequency-resolved electrical impedance measurements and finite element (FE) simulations.[16,17] This method has, inter alia, following advantages: (i) appropriate material parameters can be expected by the simulation feedback, and (ii) one sample shape is sufficient to identify the complete set of material parameters. For instance, simulated frequency-resolved electrical impedance of PZT ceramics offer better agreement with measurement results if identified material parameter set by the Inverse Method is used instead of manufacturer data.[17] Furthermore, spatially resolved surface normal velocity of a disk sample can be accurately predicted by applying the identified material parameters.[17]

NKN has high piezoelectric d constants compared with other lead-free piezoelectric materials.[3–6,10–13] There have been a lot of studies in order to further improve piezoelectric properties of NKN as well as the densification by using additives or modifying synthesis process.[3–6,10–13,18–22] In particular, it is reported that Li-modified NKN ceramics exhibits high d_{33} (>200pC/N) with remaining high T_C.[3,21,22] However, NKN have not reached PZT in terms of piezoelectric properties. Therefore, further improvement of NKN are tried by controlling its microstructure.[23] NKN offers large piezoelectric shear mode d_{15} as one of its unique properties. For example, d_{15} of NKN is 2.25 times of its d_{33} (d_{15}=189 pC/N, d_{33}=84 pC/N) value.[24] The ratio d_{15}/d_{33} of NKN is larger than that of PZT (d_{15}/d_{33}=1.47) and barium titanate $BaTiO_3$ (d_{15}/d_{33} = 1.36).[25]

Crystallographic studies of NKN crystals have also been carried out since the 1950s. The crystal structures are different from that of PZT.[25–27] Although the orthorhombic phase *Bmm*2 is stable near room temperature, NKN shows various crystal phases over a wide temperature range. The transition temperatures were estimated by *in-situ* high-temperature single-crystal diffraction measurements.[28] The orthorhombic-tetragonal phase transition temperature ($T_{O\text{-}T}$) of NKN takes place at approximately 200 °C, and tetragonal phase transits to cubic phase at approximately 400 °C. Besides, their lattice constants continuously change with temperature. Generally, the material parameters of piezoelectric materials strongly depend on their crystal structure and their spontaneous polarization direction P_s.[24] For example, the elastic stiffness constant c_{33}^E of $BaTiO_3$ is smaller than its c_{11}^E at room temperature because tetragonal phase is stable and their P_s is $[001]_{tetra}$. In addition, c_{44}^E significantly decreases by cooling to $T_{O\text{-}T}$ due to rotation of P_s to $[011]_{tetra}$. In other words, piezoelectric materials are mechanically soft along to their P_s. Most of papers about NKN have mainly focused on dielectric and piezoelectric properties, and there are only a few reports about the complete parameter set of NKN.

Here, we report on temperature dependency of the material parameters, which is still unknown but essential for practical applications of NKN. The origin of large piezoelectric shear mode d_{15} is discussed from the viewpoint of material parameters. In addition, the Inverse Method is validated by means of electric-field induced strain measurements. The manuscript is organized as follows: Section II explains the experimental procedure including material synthesis and material characterization approaches. In Sec. III, we present the obtained results at room temperature as well as the temperature dependency of the material parameters. The manuscript concludes in Sec. IV.

II. EXPERIMENTAL PROCEDURE

A. Material synthesis

NKN was synthesized through a solid-state reaction method. High purity (99.9 %) powders of Na_2CO_3, K_2CO_3 and Nb_2O_5 were weighted according to the formula $(Na_{0.55}K_{0.45})NbO_3$. These

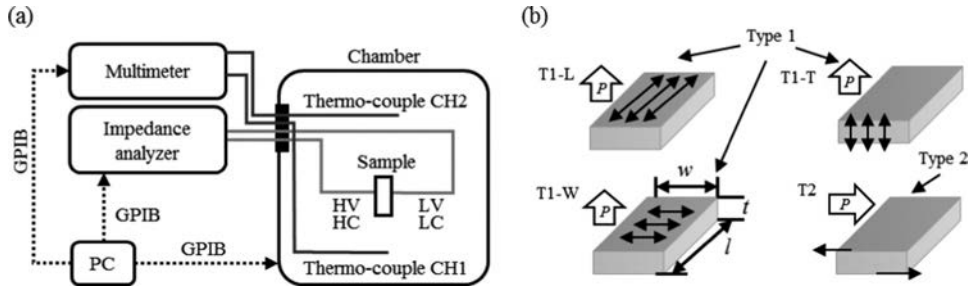

FIG. 1. (a) Experimental setup for the Inverse Method. Frequency-resolved electrical impedance of piezoceramics were measured by an impedance analyzer. Temperature of the chamber was determined by a multimeter though two thermos-couples. (b) Two different types of samples are utilized for the Inverse Method. They feature same block shape but different polarization directions: thickness direction (Type 1) and width direction (Type 2). Type 1 causes two length extensional modes (T1-L and T1-W) and one thickness extensional mode (T1-T). Thickness shear mode (T2) is caused in Type 2.

powders were mixed by wet-ball-milling for 16 h. After drying, the mixed powder was calcined at 910 °C for 10 h. Subsequently, 0.25 mol% MnO (99.9 %) powder was added to the calcined powder, and the powder was wet-ball-milled for 16 h. The dried powder was uniaxially pressed at 50 MPa and then coldisostatically pressed at 300 MPa. Sintering was carried out at 1098 °C for 2 h. The resulting NKN ceramics were cut and mirror-polished into suitable shapes. Finally, gold electrodes were formed on facing surfaces of sample and poling treatment was conducted by dc electric field of 3.0 kV/mm in silicon oil at 150 °C for 30 min.

B. The Inverse Method

The Inverse Method is an approach to identify material parameters of piezoceramics by minimizing deviation between frequency-resolved electrical impedance measurements and FE simulations.[16,17] Impedance measurements were run for two different types of samples. These samples feature the same shape (1.0×4.0×10.0 mm^3), but are polarized in different directions: thickness direction (1.0 mm: Type 1) and width direction (4.0 mm: Type 2). Experimental setup for impedance measurements is shown in Fig. 1(a). Frequency-resolved electrical impedance of each type was measured in the frequency range from 10 to 10000 kHz by an impedance analyzer. The samples were placed in a climatic chamber and temperature of the chamber was raised from 30 °C up to 150 °C. Temperature of the chamber was determined by a multimeter though two thermos-couples. To get a homogeneous temperature distribution, there was a holding time for 15 min before starting impedance measurements.[29] The measured impedance curves of Type 1 and Type 2 contain overall four distinct vibration mode resonances, which are shown in Fig. 1(b). While two length extensional modes (T1-L and T1-W) and one thickness extensional mode (T1-T) belong to Type 1, Type 2 exclusively offers a pronounced thickness shear extensional mode (T2). On the basis of these four vibration modes, the measurement results were compared with FE simulation results. In doing so, frequency-resolved electrical impedance curves were simulated with initial material parameter set provided by resonance-antiresonance method.[14] The deviations between measurement and simulation results get minimized iteratively by modifying material parameters through an optimization algorithm. Finally, the Inverse Method provides five elastic stiffness constants c_{ij}^E, two dielectric constants ε_{ij}^S, and three piezoelectric constants e_{ij} of the investigated materials. In addition, a loss factor α_{all} is determined through the Inverse Method; i.e., eleven material parameters are identified as a full parameter set.

C. Electric field induced strain measurement

Besides the frequency-resolved electric impedance, we measured the electric field induced strain in the temperature range from 25 °C up to 160 °C. Thereby, the electric field was applied in parallel to the polarization direction by using a function generator and a voltage amplifier. The

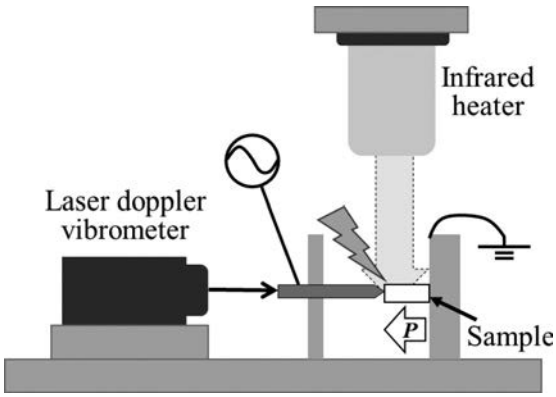

FIG. 2. Experimental setup for electric field induced strain measurement. Electric field induced strain of sample was measured by a laser Doppler vibrometer, and samples were heated up by an infrared heater.

experimental setup is shown in Fig. 2. The electric field induced longitudinal strain of the samples was measured by utilizing a laser Doppler vibrometer. The measured strain data were collected by means of a lock-in amplifier. As a heating system, an infrared heater was added. Heating rate was 3 °C/min, and there was a holding time of 10 min at each temperature step before starting the strain measurement to ensure a constant temperature. Previously, temperature calibration was performed without applied electric field by using a thermo-couple that was contacted directly the sample. An unipolar triangular wave electric field E of 500 V/mm, which is approximately half of coercive field strength of NKN, at 100 Hz was applied to the sample. The resulting piezoelectric constant d_{33} of longitudinal mode values were calculated from measured strain S according to

$$d_{33} = S/E. \tag{1}$$

To avoid influence of other piezoelectric vibration modes, we analyzed rod shaped samples ($2.0\times2.0\times4.0$ mm^3) in the framework of this method.

III. RESULTS AND DISCUSSION

A. Material constants at room temperature

The material parameters of NKN provided by the Inverse Method are listed in TABLE I. For comparison, material constants of PZT are also shown in the table. Compared with PZT, all dielectric constants and piezoelectric constants of NKN were small. In particular, dielectric constants ε_{ij}^S of NKN (e.g., ε_{11}^S=2.7×10^{-9} F/m) are smaller than one third that of PZT (e.g., ε_{11}^S=8.2×10^{-9} F/m). Three elastic stiffness constants c_{11}^E, c_{33}^E and c_{44}^E of NKN were larger than those of PZT, but the other two elastic stiffness constants c_{12}^E and c_{13}^E exhibit smaller values than PZT. It can be expected that the deviations of elastic stiffness constants between NKN and PZT are attributed to their crystal structure.[30]

TABLE I. Material constants of NKN and PZT at 30 °C. All dielectric constants and piezoelectric constants of NKN were smaller than of PZT.

	Elastic stiffness constants					Dielectric constants		Piezoelectric constants			Loss factor
Material	$c^E{}_{11}$	$c^E{}_{12}$	$c^E{}_{13}$	$c^E{}_{33}$	$c^E{}_{44}$	$\varepsilon^S{}_{11}$	$\varepsilon^S{}_{33}$	e_{31}	e_{33}	e_{15}	α_{all}
NKN	15.0	6.0	6.0	12.2	3.6	2.7	1.5	-1.0	7.1	5.9	0.01
PZT	12.3	7.7	7.0	9.7	2.2	8.2	7.6	-7.2	13.7	11.9	0.02

c_{ij}^E in 10^{10} N/m^2, ε_{ij}^S in 10^{-9} F/m, e_{ij} in C/m^2.

TABLE II. Material constants of air-sintered NKN ceramics as well as the comparison with hot-pressed NKN ceramics: (a) e-form and (b) d-form.

(a) Material	$c^E{}_{11}$	$c^E{}_{12}$	$c^E{}_{13}$	$c^E{}_{33}$	$c^E{}_{44}$	$\varepsilon^S{}_{11}/\varepsilon_0$	$\varepsilon^S{}_{33}/\varepsilon_0$	e_{31}	e_{33}	e_{15}	Reference
Air-sintered NKN	15.0	6.0	6.0	12.2	3.6	308	169	-1.0	7.1	5.9	This study
Hot-pressed NKN	19.7	10.4	10.2	16.8	3.7	545	306	-2.4	9.8	11.3	4,5,24, 25

c_{ij}^E in 10^{10} N/m^2, ε_{ij}^S in 10^{-9} F/m, e_{ij} in C/m^2.

(b) Material	$s^E{}_{11}$	$s^E{}_{12}$	$s^E{}_{13}$	$s^E{}_{33}$	$s^E{}_{44}$	$\varepsilon^T{}_{11}/\varepsilon_0$	$\varepsilon^T{}_{33}/\varepsilon_0$	d_{31}	d_{33}	d_{15}	Reference
Air-sintered NKN	8.8	-3.2	-3.2	11.3	27.6	418	244	-29	87	164	This study
Air-sintered NKN							290	-32	80		4
Hot-pressed NKN	8.2	-2.5	-3.4	10.1	27.0	938	496	-51	127	306	4,5,24, 25

s_{ij}^E in 10^{-12} N/m^2, ε_{ij}^T in 10^{-9} F/m, d_{ij} in 10^{-12} C/N.

To estimate the ratio of piezoelectric shear mode to longitudinal mode d_{15}/d_{33}, elastic compliance constants s_{ij}^E, dielectric consitants ε_{ij}^T, and piezoelectric constants d_{ij} were calculated from the constants of TABLE I according to IEEE standard.[22] The calculated material parameters are summarized in TABLE II. The obtained ratio d_{15}/d_{33} of NKN was 1.89 and larger than 1.47 of PZT. Thus, the Inverse Method also confirmed the comparatively large piezoelectric shear mode of NKN. Furthermore, it is indicated that NKN is mechanically softer in shear direction than PZT. The ratio of elastic compliance constants in shear direction to that in longitudinal direction s_{44}^E/s_{33}^E are 2.4 and 2.2 in case of NKN and PZT, respectively. Hence, there is a hypothesis that mechanical softness in shear direction s_{44}^E causes the large piezoelectric shear mode d_{15} of NKN, i.e., d_{15}/d_{33} of NKN should be proportional to their s_{44}^E/s_{33}^E.

On the other hand, the identified material parameters of normal air-sintered NKN ceramics were different from the results of hot-pressed NKN ceramics.[11,12,31,32] In e-form, all material parameters identified in this study were small compared with hot-pressed NKN ceramics. For example, c_{11}^E w15 15.0×10^{10} N/m^2 in this study, but c_{11}^E of hot-pressed NKN ceramics was 19.7×10^{10} N/m^2. The material density of the samples should be the reason for the different material parameters.[33] Relative density of NKN ceramics was approximately 97 % in this work and lower compared with hot-pressed NKN ceramics, which feature relative density greater than 99 %. Owing to the lower density, dielectric constant ε_{33}^S and piezoelectric constants e_{ij} apparently became smaller compared with hot-pressed NKN ceramics. Moreover, it could be assumed that the material became mechanically soft because low relative density ceramics have many pores inside, which means c_{ij}^E takes small values. Actually, the piezoelectric constants d_{31} and d_{33} were almost the same as previous reported with air-sintered NKN ceramics,[11] as shown in TABLE II. The relative dielectric constant $\varepsilon_{33}^T/\varepsilon_0$ got smaller due to hardening effect of doped MnO.[34] For these reasons we can conclude that a reliable material parameter set of NKN ceramics was identified by the Inverse Method.

B. Temperature dependency of material constants

Fig. 3 depicts measured electrical impedance curves of NKN at each temperature step. The impedance curves of all vibration modes shifted to lower frequency and lower impedance with increasing temperature. Moreover, resonance peaks became smaller from 30 °C up to 120 °C, but got larger at 150 °C compared with 120 °C. The resonance pairs showed almost the same impedance range at 30 °C and 150 °C. Based on these impedance curves, we identified the material parameters at each temperature step.

The resulting material parameters of NKN as a function of temperature are displayed in Fig. 4. Dielectric constants ε_{ij}^S increased monotonously, which means NKN became electrically soft near their phase transition temperature. In addition, the dielectric constants showed isotropic increase. Dielectric constant ε_{11}^S vertical to polarization direction increased by 32 % from 30 °C up to 150 °C.

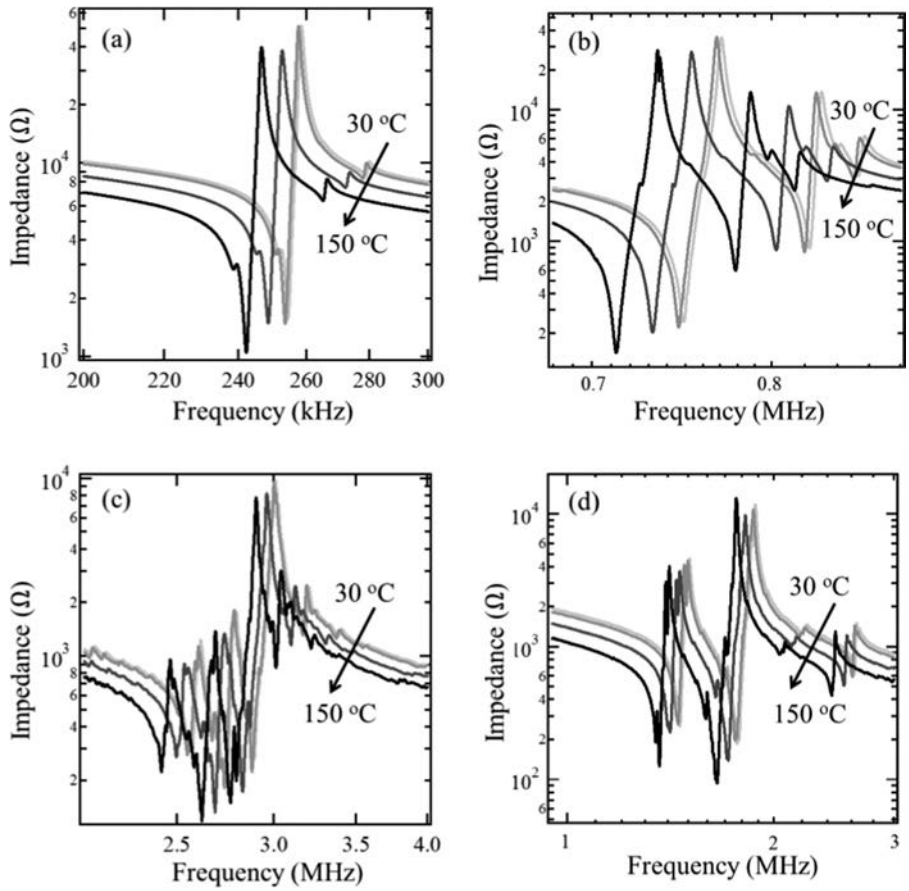

FIG. 3. Measured electrical impedance curves of NKN at each temperature step: length extensional modes (a) T1-L and (b) T1-W, (c) thickness extensional mode T1-T, and (d) thickness shear extensional mode T2.

Dielectric constant ε_{33}^S, which is parallel to poling direction, showed similar behavior like ε_{11}^S since a 29 % increment of ε_{33}^S was observed in the investigated temperature range. The increment of dielectric constants improved the piezoelectric constants e_{ij}, which also increased monotonously with rising temperature except e_{31}. The behavior of piezoelectric coupling constants e_{33} and e_{15} agreed very well with each other: both increased 14 % from 30 °C to 150 °C. In fact, e_{31} should offer similar behavior as the other piezoelectric constants e_{33} and e_{15}. It seems that the difference in behavior between e_{31} and the other constants was caused due to instability of impedance measurements or inhomogeneity in sample material. Loss factor α_{all} showed a local maximum peak at

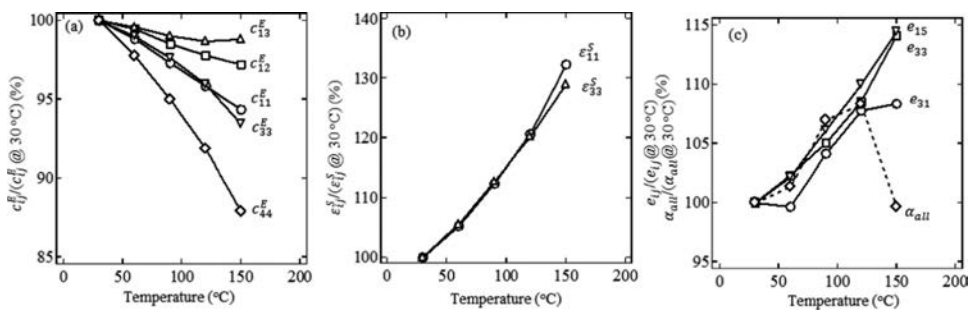

FIG. 4. Temperature dependency of material constants for NKN. (a) elastic stiffness constants, (b) dielectric constants, and (c) piezoelectric coupling constants as well as loss factor. All dielectric and piezoelectric constants increased with increasing temperature, but elastic stiffness constants showed anisotropic decrease.

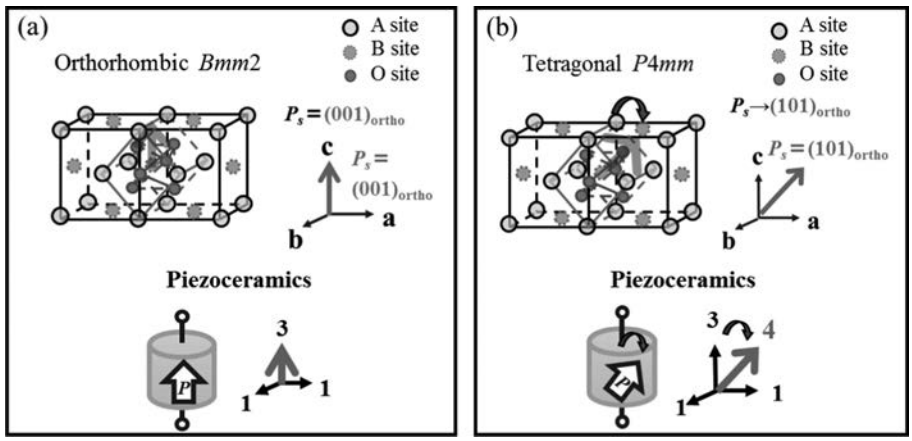

FIG. 5. Crystal structure and spontaneous polarization direction P_s of NKN at (a) 30 °C and (b) 150 °C. While orthorhombic phase transits to tetragonal phase, P_s rotates from $[001]_{ortho}$ to $[101]_{ortho}$ and, consequently, global polarization direction of piezoceramics also rotates.

approximately 120 °C, and returned almost to the initial value of 30 °C at 150 °C. This temperature dependency should be associated with the impedance range of resonance pairs. In the other words, if α_{all} rises, the impedance range becomes small.

The elastic stiffness constants c_{ij}^E monotonously decreased with increasing temperature, which means NKN becomes also mechanically soft near their phase transition temperature. However, this decrease differs remarkably. For example,c_{13}^E decreased only less than 2 %, but c_{44}^E decreased approximately 12 % from 30 °C to 150 °C. The temperature behavior of c_{44}^E can be explained in terms of crystal structures and direction P_s of spontaneous polarization. As mentioned above, the crystal structure of NKN is a orthorhombic *B*mm2 system and P_s is $[001]_{ortho}$ at room temperature. As shown in Fig. 5(a), P_s coincides with polarization direction of piezoceramics. It can be assumed that piezoceramics are mechanically soft in polarization direction. Actually, elastic stiffness constant c_{33}^E parallel to polarization direction of NKN is smaller than that vertical to polarization direction c_{11}^E at room temperature (c_{11}^E=15.0×10^{10} N/m^2, c_{33}^E=12.2×10^{10} N/m^2). Up to 150 °C, the temperature of sample approached $T_{O\text{-}T}$, and the crystal phase became similar to tetragonal phase. Due to phase transition, P_s also rotated from $[001]_{ortho}$ to $[101]_{ortho}$. In case of piezoceramics, the rotation of P_s should mean apparent rotation of polarization direction from longitudinal direction to shear direction, as shown in Fig. 5(b). Thus, NKN became mechanically softer in shear direction while temperature increased and c_{44}^E decreased significantly. To confirm proportional relationship between s_{44}^E/s_{33}^E and d_{15}/d_{33}, they were calculated at each temperature step. FIG 6 contains the values of s_{44}^E/s_{33}^E and d_{15}/d_{33} as a function of temperature. The value of s_{44}^E/s_{33}^E increased with increasing temperature, and showed a local maximum 2.49 at 120 °C. With further temperature increment, s_{44}^E/s_{33}^E slightly decreased. As expected, d_{15}/d_{33} showed similar temperature dependent behavior to s_{44}^E/s_{33}^E. The ratio d_{15}/d_{33} increased from 1.89 to 1.96 up to 120 °C. After reaching a local maximum value at 120 °C, d_{15}/d_{33} decreased down to 1.94 at 150 °C. This suggests that mechanical softness of NKN in shear direction is one of the origins of large piezoelectric shear mode d_{15}.

Fig. 7 depicts the temperature dependency of d_{33} determined by two different methods: (a) electric field induced strain measurement method, and (b) the Inverse Method. Both methods yield a monotonous increase of d_{33}. In case of electric field induced strain measurement method, the d_{33} value increased from 72.9 pm/V to 96.3 pm/V in the temperature range from 23 °C up to 160 °C, which means 32 % increment. According to the results of the Inverse Method, the d_{33} value increased from 86.5 pC/N to 109.8 pC/N from 30° C up to 150 °C, which equals 26 % increment. In particular, this value increased significantly after 120 °C: 14 % increment from 126 °C to 160 °C in case of electric field induced strain measurement method and 11 % increment from 120 °C to 150 °C for Inverse Method. The temperature dependency from the Inverse Method

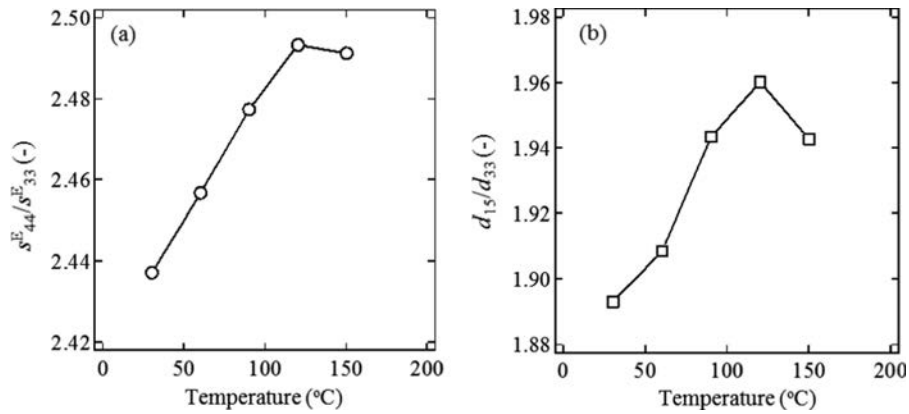

FIG. 6. (a) Ratio of elastic compliance constants s^E_{44}/s^E_{33} and (b) piezoelectric constants d_{15}/d_{33} as a function of temperature. Both s^E_{44}/s^E_{33} and d_{15}/d_{33} increased with rising temperature except for 150 °C, and showed similar temperature dependency to each other.

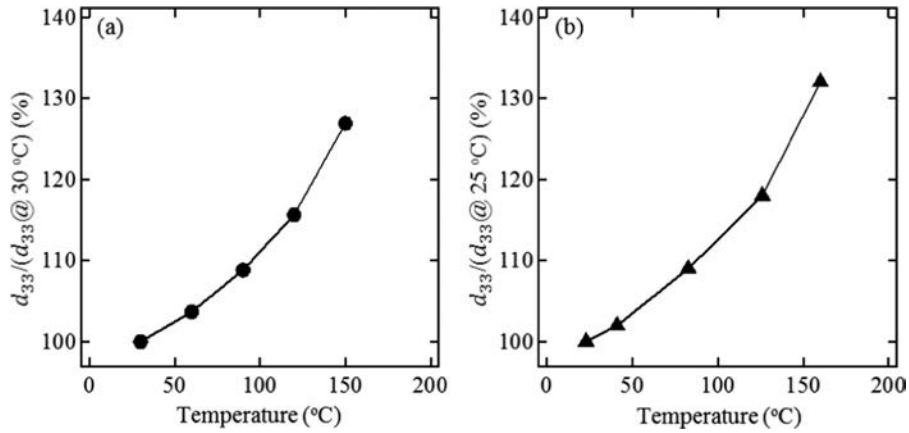

FIG. 7. (a) Temperature dependency of piezoelectric longitudinal constant d_{33} as a function of temperature characterized by the Inverse Method and (b) electric field induced strain measurement method.

didn't completely agree with that from electric-field induced strain measurement method. The deviation between two methods would be associated with different amplitude of applied electric field.[35] It is reported that d_{33} increases with increasing temperature more under high electric field than under low electric field because of non-180 ° domain wall motions. We could concluded that the deviation between two methods was small enough to prove high reliability of the Inverse Method in the investigated temperature range. Deviations of the absolute values between both methods would be caused due to different measurement principles, various samples and measurement conditions, such as frequency and amplitude of applied electric field.[36–38]

IV. CONCLUSION

We exploited the simulation-based Inverse Method to characterize material parameters of NKN. All dielectric ε^S_{ij} and piezoelectric constants e_{ij} increased monotonously as well as isotropically with respect to temperature. Elastic stiffness constants of NKN showed anisotropic decrease while temperature raised because temperature of sample approached their orthorhombic-tetragonal phase transition temperature $T_{\text{O-T}}$, which is approximately 200 °C. Large piezoelectric shear mode d_{15} of NKN was confirmed also by the Inverse Method. Furthermore, it was identified that NKN is mechanically soft in shear direction in comparison with s^E_{44}/s^E_{33} of PZT. Both d_{15}/d_{33} and s^E_{44}/s^E_{33} of NKN showed similar temperature dependent behavior, which indicate that the mechanical softness

in shear direction should be one of the origin of the large piezoelectric mode d_{15}. Thus, piezoelectric properties of NKN ceramics depend on their mechanical properties such as elastic stiffness constants and elastic compliance constants. Results of this study confirmed that NKN are suitable for high temperature devices. In these applications, piezoelectric materials are used not only under high temperature but also under high compressive stress. Compressive stress could influences on mechanical properties of piezoceramics and its polarization state, and interacts with temperature.[39–41] Therefore, NKN ceramics should be characterized not only under high temperature but also under high compressive stress and other environmental conditions, e.g., combined condition with high temperature and high compressive stress for their application. It is expected that the Inverse Method is a helpful approach to characterize material parameters under such conditions.

ACKNOWLEDGMENTS

This work was supported by JSPS Grant-in-Aid for Scientific Research B, JSPS Bilateral Program with DFG, and Collaborative Research Centre/Transregio 39 PT-PIESA (DFG), subproject C06.

[1] W. Heywang, K. Lubitz, and W. Wersing, *Piezoelectricity* (Springer, 2008).
[2] J. Tichy, J. Erhart, E. Kittinger, and J. Privrastka, *Fundamentals of Piezoelectric Sensorics* (Springer, 2010).
[3] Y. Saito, H. Takao, T. Tani, T. Nonoyama, K. Takatori, T. Homma, T. Nagata, and M. Nakamura, Nature **432**, 84 (2004).
[4] J. F. Li, K. Wang, B. P. Zhang, and L. M. Zhang, J. Am. Ceram. Soc. **89**, 706 (2006).
[5] Z. Y. Shen, J. F. Li, K. Wang, S. Xu, W. Jiang, and Q. Deng, J. Am. Ceram. Soc. **93**, 1378 (2010).
[6] J. S. Zhou, F. Z. Yao, K. Wang, Q. Li, X. M. Qi, F. Y. Zhu, and J. F. Li, J. Mater. Sci.-Mater. El. **26**, 9329 (2015).
[7] H. Zhang, P. Xu, E. Patterson, J. Zang, S. Jiang, and J. Rödel, J. Eur Ceram. Soc. **35**, 2501 (2015).
[8] K. Tabuchi, H. Nagata, and T. Takenaka, J. Ceram. Soc. Jpn. **121**, 623 (2013).
[9] S. Someno, H. Nagata, and T. Takenaka, J. Ceram. Soc. Jpn. **122**, 406 (2014).
[10] G. Shirane, R. Newnham, and R. Pepinsky, Phys. Rev. **96**, 581 (1954).
[11] L. Egerton and D. M. Dillon, J. Am. Ceram. Soc. **42**, 438 (1959).
[12] R. E. Jaeger and L. Egerton, J. Am. Ceram. Soc. **45**, 209 (1962).
[13] G. H. Haertling, J. Am. Ceram. Soc. **50**, 329 (1967).
[14] *IEEE Standard on Piezoelectricity*, Std., 1988.
[15] L. Tang and W. Cao, Appl. Phys. Lett. **106**, 052902 (2015).
[16] S. J. Rupitsch and R. Lerch, Appl. Phys. A-Mater. **97**, 735 (2009).
[17] S. J. Rupitsch and J. Ilg, IEEE Trans. On Ultrason., Ferrolect., and Freq. Contr. **62**, 1403 (2015).
[18] K. Kakimoto, Y. Hayakawa, and I. Kagomiya, J. Am. Ceram. Soc. **93**, 2423 (2010).
[19] Y. Kizaki, Y. Noguchi, and M. Miyayama, Appl. Phys. Lett. **89**, 142910 (2006).
[20] Y. Guo, K. Kakimoto, and H. Ohsato, Jpn. J. Appl. Phys. **43**, 6662 (2004).
[21] Y. Guo, K. Kakimoto, and H. Ohsato, Appl. Phys. Lett. **85**, 4121 (2004).
[22] K. Higashide, K. Kakimoto, and H. Ohsato, J. Eur Ceram. Soc. **27**, 4107 (2007).
[23] K. Hatano, A. Yamamoto, Y. Doshida, and Y. Mizuno, J. Ceram. Soc. Jpn. **123**, 561 (2015).
[24] R. E. Newnham, *Properties of materials: Anisotropy, Symmetry, Structure* (Oxford University Press, 2004).
[25] E. Li, Y Zhen, L. Zhang, and K. Wang, Ceram. Int. **34**, 783 (2008).
[26] B. Jaffe, W. Cook, and H. Jaffe, *Piezoelectric Ceramics* (Academic Press Limited, New York, 1971).
[27] N. Ishizawa, J. Wang, T. Sakakura, Y. Inagaki, and K. Kakimoto, J. Solid State Chem. **183**, 2731 (2010).
[28] T. Sakakura, J. Wang, N. Ishizawa, Y. Inagaki, and K. Kakimoto, IOP Conference Series: Mater. Sci. Eng. **18**, 022006 (2011).
[29] J. Ilg, S. Rupitsch, and R. Lerch, IEEE Sens. J. **13**, 2442 (2013).
[30] K. Ogo, M. Weiss, S. J. Rupistch, R. Lerch, and K. Kakimoto, in *Proceeding of 2015 IEEE International. Ultrasonics Symposium*, *Taipei, Taiwan*, *21-24 October 2015*, edited by P. C. Li (National Taiwan University, Taipei).
[31] B. Hansu, D. Damjanovic, and N. Setter, J. Eur Ceram. Soc. **26**, 861 (2006).
[32] R. Zuo, J. Rödel, R. Chen, and L. Li, J. Am. Ceram. Soc. **89**, 2010 (2006).
[33] N. M. Gokhale, S. C. Sharma, and R. Lal, B. Mater. Sci. **11**, 49 (1988).
[34] D. Lin, K. W. Kwok, and H. L. W. Chan, J. Alloy Compd. **461**, 273 (2008).
[35] M. Kiyohara, K. I. Katou, and K. Nagata, J. Ceram. Soc. Jpn **103**, 1233 (1995).
[36] T. Tsurumi, Y. Kumano, N. Ohashi, T. Takenaka, and O. Fukunaga, Jpn. J. Appl. Phys. **36**, 5970 (1997).
[37] T. Tsurumi, T. Sasaki, H. Kakemoto, T. Harigai, and S. Wada, Jpn. J. Appl. Phys. **43**, 7618 (2004).
[38] D. Damjanovic and M. Demartin, J. Phys.: Condens. Matter **9**, 4943 (1997).
[39] P. M. Chaplya and G. P. Carman, J. Appl. Phys. **90**, 5278 (2001).
[40] D. Zhou, M. Kamlah, and D. Munz, J. Eur Ceram. Soc. **25**, 425 (2005).
[41] K. G. Webber, E. Aulbach, T. Key, M. Marsilius, T. Granzow, and J. Rödel, Acta Mater. **57**, 4614 (2009).